Iranian Journal of Materials Forming 13 (4) (2026) 60-70

Online ISSN: 2383-0042

Iranian Journal of Materials Forming

Journal Homepage: http://ijmf.shirazu.ac.ir

Research Article

Finite Element Modeling of Brick Extrusion: Optimizing Die Angle for Uniform Outlet Velocity

Abolfazl Noh Rouzian and Abbas Ghaei*

Department of Mechanical Engineering, Isfahan University of Technology, Isfahan 84156-83111, Iran

ARTICLE INFO

Article history:

Received: 18 December 2025
Reviewed: 18 January 2026
Revised: 3 February 2026
Accepted: 7 June 2026

Keywords:

Brick
Extrusion
Finite element simulation
Optimization
Die design

Please cite this article as:

Noh Rouzian, A., & Ghaei, A. (2026). Finite element modeling of brick extrusion: optimizing die angle for uniform outlet velocity. *Iranian Journal of Materials Forming*, *13*(4), 60-70. https://doi.org/10.22099/IJMF.2026.55200.1367

ABSTRACT

Extrusion is a manufacturing process in which material is fed into a chamber and subjected to pressure. A die of the desired shape is placed at the exit of the chamber. The formed material exits the die and takes on the shape of the die cross-section. This study used the Herschel-Bulkley-Papanastasiou (HBP) model as the material model for simulating this process. To optimize product quality, we applied genetic algorithms to assess key parameters influencing the extrusion process, which helped us pinpoint the ideal die angle for achieving a more uniform outlet velocity distribution. The results showed that adjusting the die angle significantly improved flow uniformity, reducing velocity differences at the outlet by up to 60% compared with non-optimized dies. Finally, a physical experiment validated these findings, showing a close match with the predictions from our numerical simulations and optimization results.

1. Introduction

Extrusion is a common method for manufacturing bricks, involving the shaping of a prepared clay paste. The clay, mixed with water to achieve a plastic consistency, is fed into an extruder, a machine equipped with a die that determines the final shape of the brick. The paste is forced through the die under high pressure, emerging as a continuous column. This column is then cut into individual bricks of desired length using a wire cutter. The extruded bricks are subsequently dried and fired in a kiln to attain their final hardness and durability.

Extrusion, while efficient, can introduce defects into the brick production process. Common issues include delamination, where the clay layers within the brick separate, resulting in reduced strength. Die lines, or hairlines on the surface, can be caused by uneven flow in the die. Tearing, or irregular surface fractures, may result from poor die design or process parameters. In

* Corresponding author
E-mail address: ghaei@iut.ac.ir (A. Ghaei)
https://doi.org/10.22099/IJMF.2026.55200.1367

addition, internal defects such as voids can compromise the structural integrity of the brick. Careful control of clay consistency, extrusion pressure, and die design is critical to minimizing these defects and ensuring the production of high-quality bricks, as discussed below in the references.

Among the factors influencing extrusion, die design plays a pivotal role in determining both the quality and efficiency of the manufacturing process. A well-designed die ensures uniform flow of the clay paste, minimizing defects like lamination and tearing. The die's geometry, including the shape and size of the orifice, determines the final shape and dimensions of the extruded brick. Additionally, the die material and surface finish impact friction and wear resistance, affecting the overall production rate and the longevity of the tooling. Careful consideration of these factors is essential for optimizing the extrusion process and producing bricks that meet stringent quality standards.

Designing an extrusion die for brick manufacturing is a complex task that requires a deep understanding of clay properties, extrusion mechanics, and manufacturing constraints. The die must be robust enough to withstand high pressures and abrasive clay, yet precise enough to produce bricks with consistent dimensions and surface finish. Challenges include minimizing friction to prevent tearing and lamination, ensuring uniform flow distribution to avoid defects, and designing for optimal heat dissipation to prevent premature wear. The importance of a well-designed die cannot be overstated, as it directly impacts product quality, production efficiency, and overall manufacturing costs.

Finite element analysis of ECAP processes demonstrates that smaller die angles increase strain intensity while reducing uniformity, with channel displacement significantly improving homogeneity; material strength primarily affects pressing forces rather than strain distribution [1]. Subsequent HyperXtrude® simulations effectively predict material flow and tool stresses, though industrial implementation remains limited by computational demands and required expertise [2]. A novel 90°/ 20° ECAP die design reduces friction and improves strain homogeneity, experimentally validated through enhanced aluminum hardness and tensile properties [3]. For ceramic extrusion, rigid-viscoplastic FEM with Tresca friction laws accurately models die mandrel stresses, outperforming Coulomb friction assumptions [4]. Statistical analysis of 616 die failures reveals fracture predominance (46%) in solid dies, while hollow dies exhibit wear (36%) and deflection (33%) failures [5]. Thermal management studies identify 400 °C as the critical die temperature for preventing surface defects in semi-solid A356 extrusion, though unmodeled liquid flow causes minor filling discrepancies [6]. FEM investigations of weld chambers demonstrate that shallow designs (2-10 mm) create gas pockets and reduce seam ductility by 50%, while deeper 15 mm chambers improve bonding [7]. Thin-walled tube production benefits from mandrel tooth optimization (18.6% stress reduction) and variable bearing lengths, achieving 4.6 mm/s velocity uniformity and extended die life [8]. A coupled 3D CFD/ 2D reduced-order model enables real-time extrusion optimization with only 6% prediction error, significantly advancing process control capabilities [9]. Cold forging die optimization through FEM and Nelder-Mead algorithms reduces hardness variation by 46.8% via precise geometric parameter control [10]. For complex aluminum profiles, modified porthole dies with adjusted angles and baffles achieve exceptional flow balance (±1.6 mm/s velocity difference) [11]. Fundamental die angle studies establish 12°-17° as the optimal semi-cone range for minimizing extrusion forces [12]. Analytical models using Herschel-Bulkley rheology successfully predict paste extrusion pressures, bridging rigid-plastic and power-law fluid behaviors [13]. Ultrasonic-assisted extrusion demonstrates 12% pressure reduction and 20% faster processing while improving ceramic product density and frost resistance [14]. Advanced parameterization methods employing PSO algorithms enable precise rheological characterization from viscometer data [15]. A physics-based optimization method extracts Herschel-Bulkley parameters from pipe flow data, showing < 1% error for flow indices but -24% for yield stress, while maintaining computational efficiency [16].

Given the complexity of the extrusion process and the critical role of die design, this study aims to optimize the geometry of the extrusion die to achieve uniform velocity distribution at the die outlet, thereby minimizing defects and enhancing product quality. The finite element package COMSOL Multiphysics® was employed to simulate the extrusion process, capturing the flow behavior of the clay paste under various conditions. An objective function was defined to quantify the non-uniformity of velocity at the die exit, and the optimization was carried out using a genetic algorithm implemented in MATLAB.

To validate the computational results, a small-scale extrusion experiment was conducted using two dies: one with the optimized die angle and another with a conventional, non-optimized design. The experimental results confirmed that the optimized die significantly improved material flow uniformity, resulting in fewer defects and enhanced product quality compared to the non-optimized die. This study highlights the potential of integrating FEM and optimization algorithms to advance the design of extrusion dies for brick manufacturing, ultimately contributing to more efficient and sustainable production processes.

2. Material Model

The Herschel-Bulkley fluid model, often referred to as an extended Bingham [17] model, is a widely used constitutive equation for describing non-Newtonian fluid behavior. In contrast to Newtonian fluids, whose shear stress is linearly proportional to the shear rate, Herschel-Bulkley fluids exhibit a nonlinear relationship between shear stress and shear rate, as defined by the following expression:

$$\begin{cases} \tau \geq \tau_y,\ \tau = \tau_0 + k\dot{\gamma}^n \\ \tau \leq \tau_y,\ \dot{\gamma} = 0 \end{cases} \tag{1}$$

Where τ is the applied shear stress, τ_y is the fluid yield stress, k is the consistency parameter, n is the flow index, and $\dot{\gamma}$ is strain rate.

It has been observed from the investigations carried out in Ref. [17], that the specific Herschel-Balkely-Papanatsiou (HBP) model is used in the COMSOL software to define the dynamic viscosity. The HBP fluid model gives more possibilities to fit the experimental data than the conventional models. The dynamic viscosity model of Herschel-Balkely-Papanatsiou is as follows:

$$\mu_{app} = m\left(\frac{\dot{\gamma}}{\dot{\gamma}_{ref}}\right)^{n-1} + \frac{\tau_y}{\dot{\gamma}}\left[1 - exp\left(-m_p\dot{\gamma}\right)\right] \tag{2}$$

Where m acts as a scaling parameter which depends on the properties of the material. This equation is applicable to both yielded and unyielded regions of the fluid. m_p is an empirical parameter that controls the effect of shear strain rate on viscosity and $\dot{\gamma}_{ref}$ depends on the material property and is used to smooth the graph with the experimental data.

The equilibrium equation is solved in COMSOL by expressing the shear stress in terms of the dynamic viscosity and velocity gradient:

$$\sigma = -pI + \tau \tag{3}$$

$$\sigma = -pI + 2\mu(\dot{\gamma}) * \varepsilon(v) \tag{4}$$

$$\tau = (2\left(m\left(\frac{\dot{\gamma}}{\dot{\gamma}_{ref}}\right)^{n-1}\right) + \tau_{\frac{y}{\dot{\gamma}}}[(1 - \exp(-m_p.\dot{\gamma})]) * \varepsilon(v)) \tag{5}$$

Where σ represents the stress tensor, p is the hydrostatic pressure, τ the deviatoric stresses, I is the identity matrix, and $\varepsilon(v)$ is the velocity gradient tensor. The strain rate is actually defined as the symmetric part of the velocity gradient. By selecting the HBP dynamic viscosity model, the fluid flow during brick extrusion can be effectively simulated, capturing both the yielded and unyielded regions and providing insights into flow behavior and potential defect formation.

3. Finite Element Model

Based on the findings presented in the literature review, it is evident that comprehensive research on the issues of brick extrusion with non-symmetric die remains limited.

This study addresses this gap by employing a non-axisymmetric die and meticulously defining the initial and boundary conditions. The research simultaneously examines the influence of die angle and friction parameters on the velocity distribution of paste particles at the die outlet. The template input configuration is shown in Fig. 1 and the template output is shown in Fig. 2. Fig. 3 also shows the definition of the die angle for optimization.

The specification of boundary conditions can introduce significant variations in the Navier-Stokes equations. For the inlet, velocity components must be defined. The optimal method is to specify a velocity field using a velocity condition. In COMSOL, a velocity of 0.03 m/s is assumed for the fluid inlet at the die inlet. For single-phase flow, this serves as a natural boundary condition at the outlets:

$$\left(-pI + \mu(\nabla v + (\nabla v)^T) - \frac{2}{3}\mu(\nabla . v)I\right) n = -p_0 n \qquad (6)$$

$$\left(-pI + \mu(\nabla v + (\nabla v)^T)\right)n = -p_0 n \qquad (7)$$

Here, p represents the fluid pressure at the given point, I is the identity matrix, p_0 denotes the reference

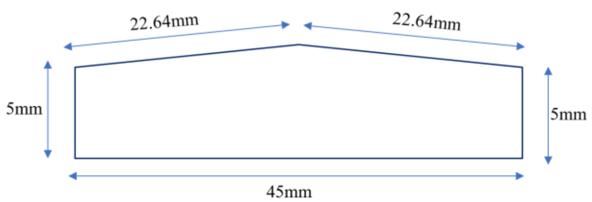

Fig. 1. Inlet cross-section of the 3D die.

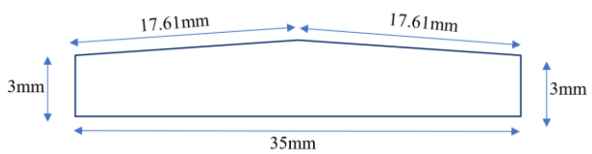

Fig. 2. Outlet cross-section of the 3D die.

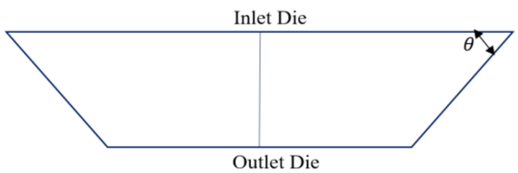

Fig. 3. Top view of the template along with showing the angle definition in the template.

pressure at the boundary point, ∇v is the velocity gradient, and n is the normal vector to the specified surface. Depending on the compressibility of the flow, the right-hand side of the above equation can be adapted to apply the pressure boundary condition for compressible, weakly compressible, or incompressible formulations. To solve this problem, another boundary condition is defined, such that the pressure at the outlet of the die is zero, which is also specified in COMSOL. This means that the right-hand side of Eq. (6) is also considered zero.

The slip condition assumes that no adhesive effects occur on the wall surface, thus preventing the formation of a boundary layer. However, the no-slip condition states that if the wall obstructs fluid movement across it, the governing relations can be formulated as follows [17].

$$v.n = 0,\ \left(-pI + \mu(\nabla v + (\nabla v)^T)\right)n = 0 \qquad (8)$$

In the above equations, relative velocity v is substituted by v_{tr}, representing the velocity of a moving wall with translational speed.

$$v_{rel} = v - v_{tr} \qquad (9)$$

Due to the high friction in the die walls, a no-slip condition has been considered for the die walls. Another important step in this simulation in COMSOL is applying meshing to the die configuration. In this software, an adaptive meshing technique and tetrahedral elements for three-dimensional problems are used for meshing. This meshing approach improves accuracy and efficiency during the numerical solution process.

4. Optimization

Optimization algorithms search for the best solution by addressing the specific constraints and requirements of a problem. The aim of this paper is to reduce the defects of the extrusion product by standardizing the speed at the exit of the die. Changes in the particle speed, caused by friction and improper die angles, can cause stress and breakage in the final product. There are various optimization algorithms such as gradient-based optimization, but one of the problems of these algorithms is that the objective function is located at local extremum points. To avoid this problem, there are solutions such as step reduction for convergence, which makes the optimization process very time-consuming, and for this reason, metaheuristic algorithms such as the genetic algorithm have been used. The advantage of this algorithm over other algorithms is that it avoids the problem of being located at local extrema due to the selection of a distinct random number. Also, compared to other metaheuristic algorithms, the genetic algorithm has the ability to optimize without initial default values. The general process of the genetic algorithm is that first, in the specified time interval for parameter optimization, the interval values are calculated as random selection and different output values are found for each of the input values according to the objective function and are ranked relative to each other. In the next step, each of the values that are in better ranks is combined with each other. The combination of the parameters occurs using changes in binary values, and then reclassification is performed. This iterative process is repeated until the output values satisfy the convergence criterion or fall below the threshold specified by the user. The genetic algorithm is available in MATLAB software, and a script is written to use MATLAB and COMSOL together so that these two software packages can be linked. This combination helps transfer the same speed and pressure data to MATLAB and to optimize the die angle with the genetic algorithm. For particles in the die inlet, a speed of 0.03 m/s is considered based on data selected from the brick extrusion industry. Based on the law of conservation of mass and the fact that the area of the die outlet is half the area of the inlet, it is expected that the speed of all particles at the die outlet will be 0.06 m/s. However, due to friction between the mud particles and the die wall, the speed of all particles at the outlet will not be 0.06 m/s. For this reason, by changing the angle, it can be seen that the velocity distribution can be optimized. Now, with the definition made, the cost function must be defined in this section. The cost function is equal to the sum of the difference in the speed of each particle at the die outlet from 0.06 m/s multiplied by its transpose to eliminate negative values, because these negative values cause errors. To use the genetic algorithm, another step is needed called the stopping criterion of the genetic algorithm. In this section, it is written that after 100 generations of iteration, the best solution is selected as the parameter set that minimizes the cost function. All the steps mentioned are shown schematically in Fig. 4.

5. Physical Modeling

To validate the numerical simulation results, an experimental setup was built for conducting lab-based extrusion tests. A die was created using the fused deposition modeling (FDM) process with polylactic acid (PLA) filament, chosen for its machinability, pressure resistance, and cost-effectiveness. Fig. 5 presents the

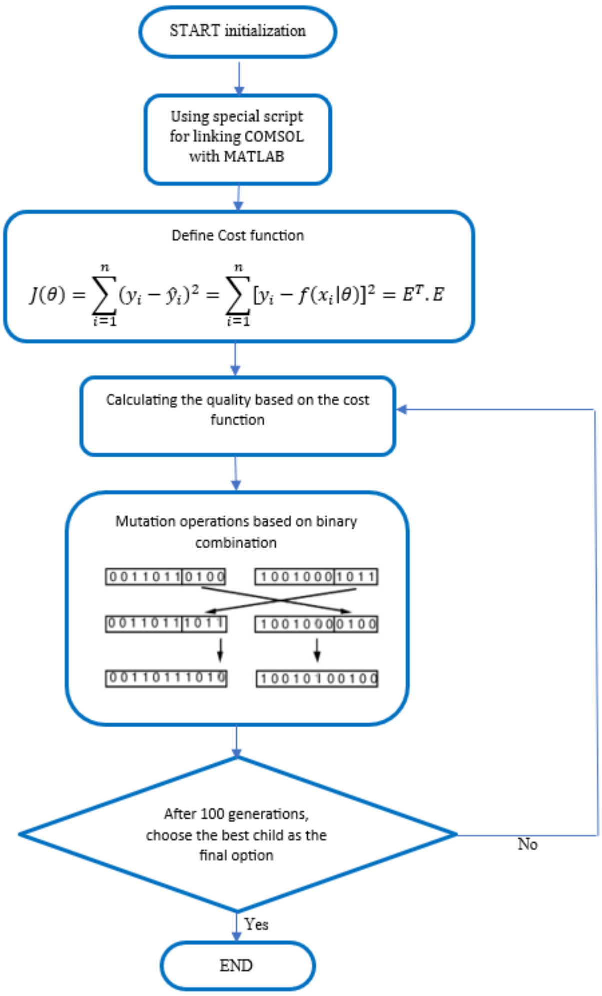

Fig. 4. Schematic representation of the optimization process and the integration of COMSOL and MATLAB.

isometric view of the prototype, while Fig. 6 shows a cross-sectional view of the device.

To ensure a constant extrusion rate, the setup was mounted on a lathe. As illustrated in Fig. 7, the assembly was securely clamped in the lathe chuck, and the piston was driven by the carriage. The lathe was configured to a tool feed speed of 0.03 m/s, resulting in a consistent piston travel speed.

For the paste mixture, 800 g of clay and 200 g of water were blended for 15 minutes using an electric mixer at a constant speed. This process prevented clay particle separation and ensured a homogeneous mixture. The paste was then loaded into the cylinder and extruded through the die outlet by the piston.

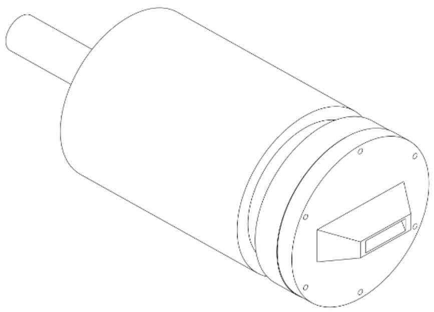

Fig. 5. Isometric view of the constructed physical simulation device.

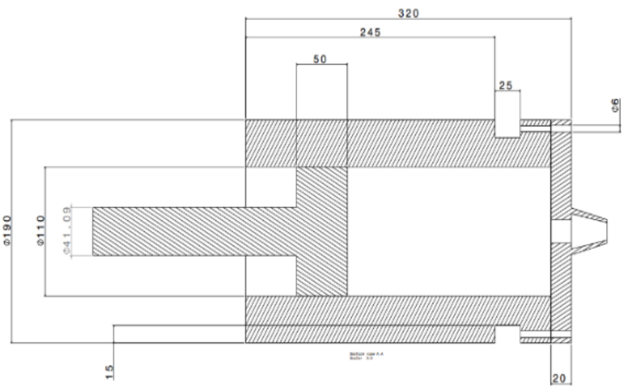

Fig. 6. Cross-sectional view of the constructed physical simulation device (dimensions in mm).

Fig. 7. The mounting mechanism of the physical simulation apparatus within the lathe system.

6. Results and Discussion

6.1. Identification of material model parameters

A rheometer is a laboratory instrument used to measure various rheological properties, including dynamic viscosity, strain rate, and shear stress. Unlike conventional viscometers, rheometers can measure a wider range of material behaviors. In this study, an MCR 302 rheometer was employed. This instrument operates by measuring the power required to rotate a stirrer within a sample. This measurement allows for the determination of parameters such as dynamic viscosity. The MCR 302 machine can perform tests within a strain rate of 0.1 to 1500 (1/s). Additionally, the instrument offers control over two significant parameters: temperature and time. For this study, the ambient temperature was assumed to be 25 °C.

Time, however, is another critical parameter, as each solution or paste has a specific time range for determining its rheological properties. Beyond this time range, the material's behavior may change significantly. For example, clay contains moisture from water, and if it remains at ambient temperature for too long, the material becomes brittle, losing its fluidity. Furthermore, friction between the tested clay and the rheometer plate causes an increase in temperature, leading to evaporation of the clay moisture. Therefore, it is essential to select an appropriate time, which varies for different types of clay. Based on repeated experiments and the observed chart in Figs. 8 and 9, it was found that, for this specific clay, viscosity decreased with increasing shear rate, while shear stress increased with shear rate in the HBP fluid model. For this specific clay, an optimal time of 2 minutes was determined [15].

A rheometer test is conducted under controlled shear conditions, allowing strain rate $\dot{\gamma}$ to be represented by a single scalar value, which serves as the input parameter in the HBP equation. The output data (shear stress) is then recorded. To ensure the reliability of the results obtained, this experiment is repeated several times. The

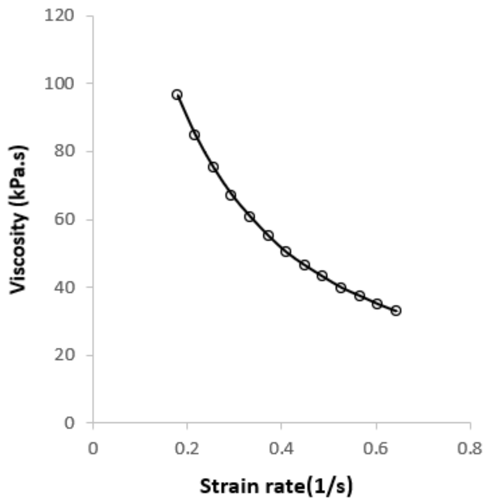

Fig. 8. Variations in empirical viscosity with respect to strain rate.

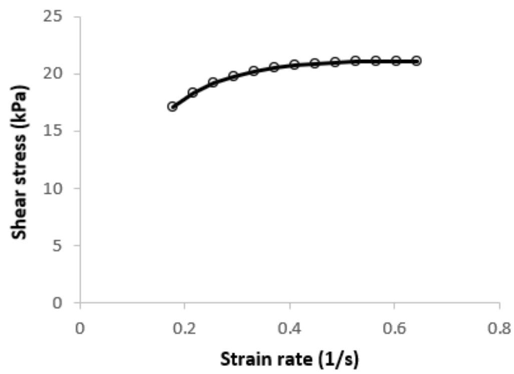

Fig. 9. Variations in empirical strain rate with respect to shear stress.

experiments performed and the data recorded after ensuring the consistency of successive experiments are shown in Fig. 9.

As can be seen from Figs. 8 and 9, the changes in shear stress and dynamic viscosity as a function of strain rate were extracted from the experimental test using a rheometer. In a rheometer test, the material is subjected to controlled shear, and the sample undergoes deformation due to the applied shear stress. In this case, the velocity gradient can be considered as the strain rate and a scalar number. Because the deformation caused by loading is a change in a uniform deformation in the direction of loading. Therefore, Eq. (5) can be rewritten as Eq. (10). We have the data of uniaxial shear stress and dynamic viscosity in terms of different strain rates and we want to fit the five unknown coefficients of the HBP fluid model including m, $\dot{\gamma}_{ref}$, n, τ_y, m_p with these data and the HBP fluid model in a way that makes it consistent with the experimental data. To extract the parameters of the HBP fluid model, the generalized reduced gradient algorithm is used to solve nonlinear optimization problems, which is a type of data fitting algorithm. This algorithm is particularly effective for nonlinear programming problems involving nonlinear constraints. This algorithm is available in Microsoft Excel. First, the experimental data are imported into the software and then the HBP fluid model is defined. The experimental data extracted from Fig. 9 were subsequently imported into Microsoft Excel for further analysis. Then, the reduced gradient algorithm is used to extract the parameters of the HBP fluid model for this optimization problem. Among the algorithms tested in Excel, the generalized reduced gradient algorithm showed the best performance for optimizing the data obtained from the HBP fluid model. Fig. 10 compares the experimental data with the data obtained using the generalized reduced gradient algorithm, which has the lowest error with the experimental data. Also, in Table 1, you can see the parameters extracted from the generalized reduced gradient algorithm.

$$\tau = (2\left(m\left(\frac{\dot{\gamma}}{\dot{\gamma}_{ref}}\right)^{n-1}\right) + \tau_{\frac{y}{\dot{\gamma}}}[(1 - \exp(-m_p.\dot{\gamma})]]) * \dot{\gamma}) \quad (10)$$

6.2. Finite element simulation

To simulate the axially asymmetric brick extrusion process in COMSOL software, it is necessary to define the HBP fluid model parameters precisely, which are presented in Table 1. After this step, the die is drawn, and the inlet and outlet openings are shown in Figs. 1 and 2. The angle definition is also shown in Fig. 3 and is defined as an unknown parameter in COMSOL software for optimization. All boundary conditions are defined in accordance with section 2. After all these steps and linking COMSOL software with MATLAB to use the genetic algorithm, the results are obtained for different die angles, which are shown in Figs. 11 and 12, for two different angles, and after the optimization of the die angle parameter, the optimal result is shown in Fig. 14.

Table 1. Material parameters for the elastic part of the proposed constitutive model

HBP model parameter	ρ (kg/m^3)	τ_y (N/m^2)	n	$\dot{\gamma}_{ref}$ $(1/s)$	m $(Pa.s)$	m_p
Parameter value	1340	10589	0.8	101.2	97.86	0.5

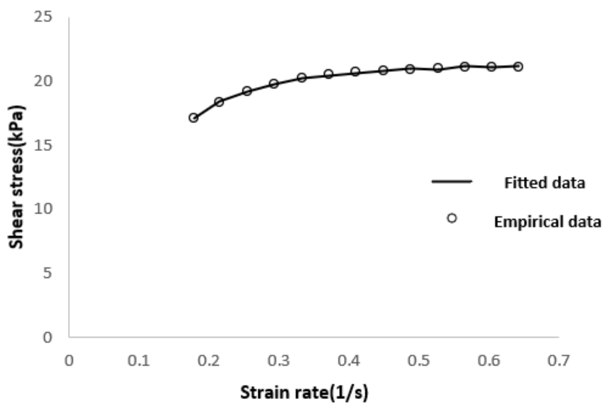

Fig. 10. Comparison of the experimental shear stress rate curve with the model.

6.3. Optimization of the die angle for non-axisymmetric modeling

The optimization of the die angle for non-axisymmetric modeling at an input velocity of 0.03 m/s is shown in Fig. 14. Also, Fig. 13 shows the variation of the cost function error at different die angles.

From the die outlet velocity contour results in Figs. 11 to 14, it can be concluded that as the die angle increases, the mud particles exit with the smallest speed difference relative to each other. However, it should be noted that by increasing the die angle, the length of the die opening also increases, which increases the friction between the mud particles and the die wall. Therefore, there is an optimal angle between 45° and 115°, which is shown in Fig. 14 for a die angle of 68°.

6.4. Physical modeling

To validate the optimization results, two dies were fabricated: one with an optimized angle of 68 degrees and another with a 48-degree angle. Extrusion trials were conducted under identical conditions for both dies. Fig. 15 illustrates the extrusion exit condition of the clay from the die, while Fig. 16 displays the corresponding velocity distribution in the finite element simulation. As observed, the clay exits in a discontinuous and irregular

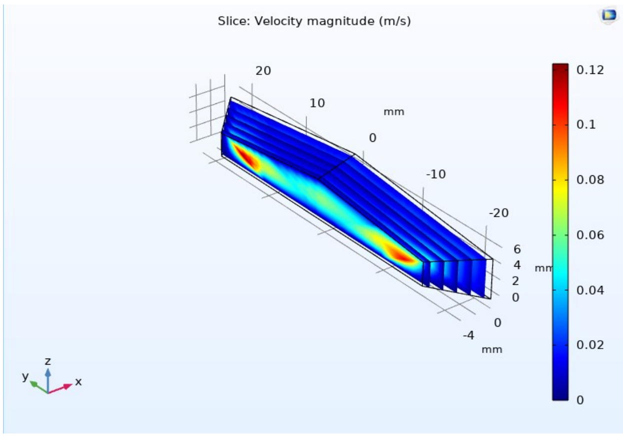

Fig. 11. Velocity distribution at a die angle of 45 under no-slip conditions.

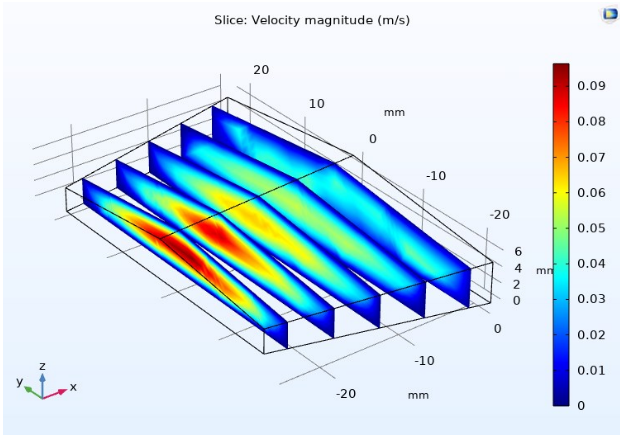

Fig. 12. Velocity distribution in 75 die angle degree and non-slip condition.

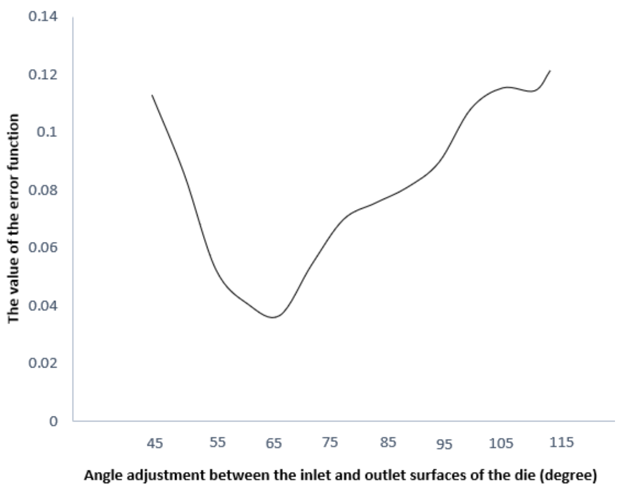

Fig. 13. Effect of die angle on reducing particle velocity differences at the outlet.

manner, indicating a non-uniform velocity distribution at the die exit. This uneven velocity profile includes shear stress in the extruded product, compromising its final quality. In contrast, Fig. 17 demonstrates the exit condition for clay extruded through the optimized die, and Fig. 18 shows the corresponding velocity distribution in the finite element simulation for the optimized die. As seen in Fig. 17, the product extruded from the optimized die exits uniformly with a consistent appearance. A comparison of Figs. 16 and 18 reveals that the velocity distribution at the exit of the optimized die is significantly more uniform than that of the non-optimized die, confirming the consistency between the finite element simulation results and the physical tests.

These findings confirm the successful application of the finite element model in conjunction with the genetic optimization algorithm. The non-uniform velocity distribution of clay particles at the die outlet, as predicted by the finite element simulation, is minimized. This results in a final product with a more uniform structure.

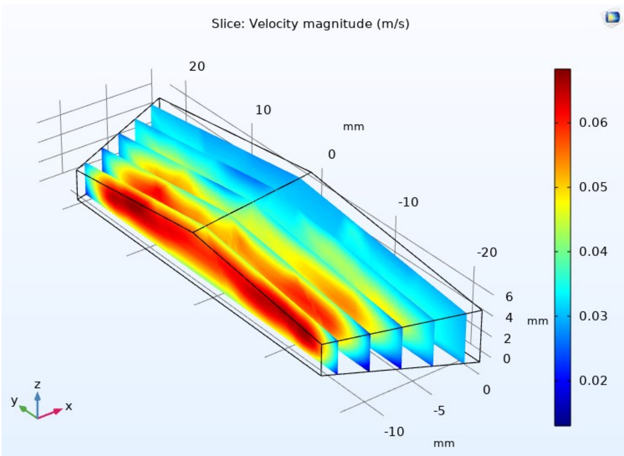

Fig. 14. Velocity distribution contour for the optimized non-axisymmetric die angle of 68°.

Fig. 15. Clay extrusion output from the non-optimized die.

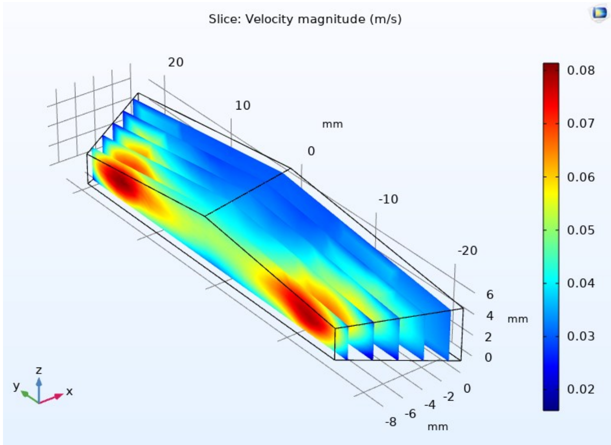

Fig. 16. Velocity distribution of the non-optimized die.

Fig. 17. Clay extrusion output from the optimized die.

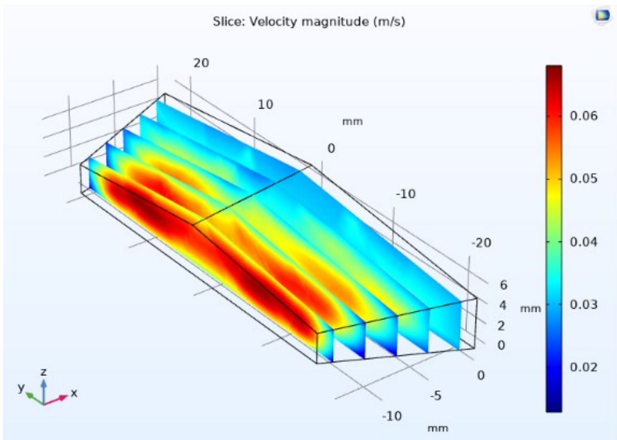

Fig. 18. Velocity distribution of the optimized die.

7. Conclusion

In this study, the defects in the brick extrusion process caused by non-uniform velocity distribution at the die outlet were investigated. Considering the complexity of the simulation process and the effect of various parameters on the velocity gradient of clay particles, the commercial finite element software COMSOL was used in combination with the Herschel-Bulkley-Papanastasiou (HBP) model. The die angle was identified as the critical parameter for optimization in three-dimensional axisymmetric problems to reduce velocity gradients. It was observed that increasing the die angle facilitates the flow of clay particles through the outlet, which reduces velocity non-uniformity. However, this increase in angle necessitates an increase in the die length, which in turn increases the friction between the die wall and the clay particles. Consequently, an optimal die angle was found within the range of 45° to 95°. To identify the optimal die angle in three-dimensional analyses, a genetic optimization algorithm was implemented. After identifying the ideal die angle, experimental trials were performed to validate the results using optimized and non-optimized die geometries. The findings confirmed the consistency between finite element simulations, genetic algorithm results, and experimental observations.

Acknowledgments

The authors would like to thank all individuals who contributed to this work through valuable discussions and suggestions, particularly the personnel of Nama-Chin Brick Company.

Authors' contributions

A. Noh Rouzian: Methodology, Material preparation, Data collection & analysis, Simulations, Experiments, Writing - original draft preparation

A. Ghaei: Conceptualization, Methodology, Supervision, Data analysis, Writing - review & editing

Conflict of interest

The authors declare that they have no known competing financial interests or personal relationships that could have appeared to influence the work reported in this paper.

Funding

No funding or external support was received for this research.

Data availability

The data that support the findings of this study are available from the corresponding author upon reasonable request.

8. References

[1] Djavanroodi, F., & Ebrahimi, M. (2010). Effect of die parameters and material properties in ECAP with parallel channels. *Materials Science and Engineering: A*, *527*(29), 7593-7599. https://doi.org/10.1016/j.msea.2010.08.022

[2] Engelhardt, M., Kurmajev, S., Maier, J., Becker, C., & Hora, P. (2019). The application of FEA for optimization of die design. *Materials Today: Proceedings*, *10*, 226-233. https://doi.org/10.1016/j.matpr.2018.10.400

[3] Surendarnath, S., Subbiah, R., Sankaranarayanasamy, K., & Ravisankar, B. (2017). Finite element simulation of pure aluminum processed by ECAP using new die design. *Materials Today: Proceedings*, *4*(2), 2544-2553. https://doi.org/10.1016/j.matpr.2017.02.108

[4] Bouzakis, K. D., Efstathiou, K., Paradisiadis, G., & Tsouknidas, A. (2008). Experimental and FEM-supported investigation of wet ceramic clay extrusion for the determination of stress distributions on the applied tools' surfaces. *Journal of the European Ceramic Society*, *28*, 2117-2127. https://doi.org/10.1016/j.jeurceramsoc.2008.02.027

[5] Arif, A. F. M., Sheikh, A. K., & Qamar, S. Z. (2003). A study of die failure mechanisms in aluminum extrusion. *Journal of Materials Processing Technology*, *134*(3), 318-328. https://doi.org/10.1016/S0924-0136(02)01116-0

[6] Choi, J. C., Park, J. H., & Kim, B. M. (2000). Finite element analysis of the combined extrusion of semi-solid material and its experimental verification. *Journal of Materials Processing Technology*, *105*(1), 49-54. https://doi.org/10.1016/S0924-0136(00)00575-6

[7] Den Bakker, A., Werkhoven, R. J., Sillekens, W. H., & Katgerman, L. (2014). The origin of weld seam defects related to metal flow in the hot extrusion of aluminum alloys EN AW-6060 and EN AW-6082. *Journal of Materials Processing Technology*, *214*, 2349-2358. https://doi.org/10.1016/j.jmatprotec.2014.05.001

[8] Fang, W., Tang, D., Wang, H., Li, D., & Peng, Y. (2019). Optimization of die design for thin-walled flat multi-port tube with the aid of finite element simulation. *Journal of Materials Processing Technology*, *277*, 116418. https://doi.org/10.1016/j.jmatprotec.2019.116418

[9] Olofsson, E. H., Dan, A., Roland, M., Jokil, N., Ramachandran, R., & Hattel, J. (2024). Numerical modeling of fill-level and residence time in starve-fed single-screw extrusion: A dimensionality reduction study from a 3D CFD model to a 2D convection-diffusion model. *The International Journal of Advanced Manufacturing Technology*, *132*, 1-15. https://doi.org/10.1007/s00170-024-13378-1

[10] Tumer, H., & Sonmez, F. O. (2009). Optimum shape design of die and preform for improved hardness distribution in cold forged parts. *Journal of Materials Processing Technology*, *209*(3), 1538-1549. https://doi.org/10.1016/j.jmatprotec.2008.04.017

[11] Wang, X., Sun, K., Liu, Z., Li, L., Li, S., & Li, F. (2021). A novel protection-type porthole die for manufacturing multi-cavity and thin-walled extrusion profile: Numerical simulation, optimization design, and experimental validation. *The International Journal of Advanced Manufacturing Technology*, *116*(5), 1691-1706. https://doi.org/10.1007/s00170-021-07582-6

[12] Yanran, Z., Wang, Z. R., & Weimin, C. (1995). Numerical simulations for extrusion and ironing and die-angle optimization. *Journal of Materials Processing Technology*, *55*(1), 48-52. https://doi.org/10.1016/0924-0136(95)01811-5

[13] Basterfield, R. A., Lawrence, C. J., & Adams, M. (2005). On the interpretation of orifice extrusion data for viscoplastic materials. *Chemical Engineering Science*, *60*, 2599-2607. https://doi.org/10.1016/j.ces.2004.12.019

[14] Faseeva, G. R., Nafikov, R. M., Lapuk, S. E., Zakharov, Y. A., Novik, A. A., Vjuginova, A. A., Kabirov R. R., & Garipov, L. N. (2017). Ultrasound-assisted extrusion of construction ceramic samples. *Ceramics International*, *43*(9), 7202-7210. https://doi.org/10.1016/j.ceramint.2017.03.008

[15] Chauhan, G., Verma, A., Das, A., & Ojha, K. (2018). Rheological studies and optimization of Herschel-Bulkley flow parameters of viscous karaya polymer suspensions using GA and PSO algorithms. *Rheologica Acta*, *57*(3), 267-285. https://doi.org/10.1007/s00397-017-1060-x

[16] Magnon, E., & Cayeux, E. (2021). Precise method to estimate the Herschel-Bulkley parameters from pipe rheometer measurements. *Fluids*, *6*, 157. https://doi.org/10.3390/fluids6040157

[17] COMSOL Multiphysics. (2020). *Polymer Flow Module User's Guide* (Version 5.6).